A synthesis of sea water pCO_2 along the western coast of the Americas

Alba Marina Cobo Viveros, Marine Research Institute (IIM-CSIC, Vigo, Spain) and University of Vigo (Vigo, Spain)

Francisco Chavez

Summer 2013

Keywords: pCO_2, Preformed nitrate, Upwelling, Western coast of the Americas, Climate change.

ABSTRACT

In order to improve the area and time coverage of seawater pCO_2 ($pCO_{2\ sw}$) observations along the eastern Pacific coast, MBARI's and LDEO's pCO_2 databases were merged and averaged by cruise and 5-degree latitudinal bins. After extracting the first 100 km from coast, a final pCO_2 database close to one million underway observations was obtained, with data from 418 cruises distributed along the Pacific coast of the Americas from Alaska to Chile. Higher pCO_{2sw} values were found in the tropics (~500 ppm) compared to pCO_{2sw} at high latitudes (~250-300 ppm). On the other hand, wind speeds were found to be lower near the tropical zone (~3 m/s) compared to high latitudes (> 6m/s). High CO_2 fluxes into the ocean were found at high latitudes (reaching -10 mol m^{-2} y^{-1} near the tip of Chile) and lower CO_2 fluxes to the atmosphere were found in the Peruvian and Chilean upwelling systems (+4 mol m^{-2} y^{-1}). In order to explain the pattern of pCO_{2sw} found for the western coast of the Americas, we correlated preformed nitrate ($NO_{3\ pre}$) values of surface waters with the pCO_2 disequilibrium (ΔpCO_2),

finding a strong and negative correlation ($r = -0.71$, $p<0.01$). Using these preformed nitrate values, we modeled a water mass from its formation, sinking, travel and upwelling in three different scenarios of nutrient utilization. We found that when no nitrate is used, $pCO_{2\ sw}$ rises to high levels in areas surrounding the tropics. This increase in $pCO_{2\ sw}$ would decrease pH, thus increasing levels of ocean acidification to higher levels than what we are presently seeing.

INTRODUCTION

Since the beginning of the industrial revolution, atmospheric CO_2 concentrations have raised from around 277 ppm in 1750 (IPCC 2007) to a global average of around 388 ppm in 2010 (Figure 10), due to the release of carbon dioxide from humankind's combined industrial and agricultural activities (Feely *et al.* 2009). The equilibration of atmospheric CO_2 with the surface ocean has been steadily decreasing seawater pH, which has increased ocean acidification during the last decades.

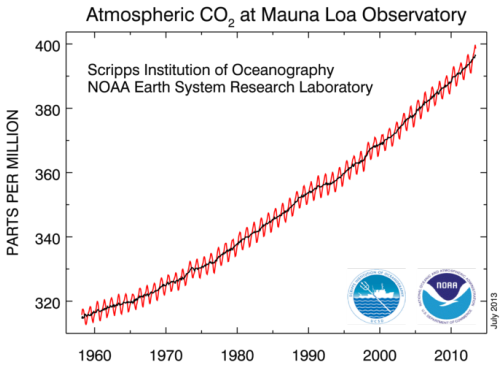

Figure 1. Keeling curve showing carbon dioxide data (red curve) on Mauna Loa, the longest record of direct measurements of CO_2 in the atmosphere (measured as the mole fraction of CO_2 in dry air). The black curve represents the seasonally corrected data. C. David Keeling of the Scripps Institution of Oceanography started these measurements in March of 1958 at a facility of the National Oceanic and Atmospheric Administration (Keeling *et al.* 1976). NOAA started its own CO_2 measurements in May of 1974, and they have run in parallel with those made by Scripps since then (Thoning *et al.* 1989). Data are reported as the dry mole fraction of CO_2, defined as the number of molecules of carbon dioxide divided by the number of molecules of dry air multiplied by one million (ppm). Source: (US Department of Commerce *et al.* 2013).

Coastal oceans, defined as the regions located 100 km from shore (Liu *et al.* 2000; Chavez *et al.* 2007) help mitigate this increase by exchanging CO_2 between the ocean, atmosphere and terrestrial environments. These and other processes modify the partial pressure of CO_2 (pCO_2) in coastal surface waters (Chavez *et al.* 2007), which is one of the reasons why these ecosystems play an important role in the global carbon cycle. However, the estimate of sea-air CO_2 fluxes in coastal waters is subject to large uncertainties (Chen and Borges 2009) due to observation limitations, large variations over small spatial and temporal scales (Liu *et al.* 2000) and rapid shift of carbon flows (Gypens *et al.* 2009). As a result, the coastal ocean has not been integrated into the global CO_2 flux calculations.

This variation over spatial and temporal scales is reflected on the existing disagreement as to whether these regions act as sources or sinks of atmospheric CO_2. Recent works have focused on the role that the coastal ocean has on sea-air CO_2 fluxes, showing uptake of atmospheric CO_2 by wind-driven upwelling margins (Hales *et al.* 2005; Cobo-Viveros *et al.* 2013), exportation of CO_2 to the deep ocean by continental margins (Tsunogai *et al.* 1999), and the importance of preformed nutrients on the role of the coastal ocean as a CO_2 sink (Hales *et al.* 2005; Friederich *et al.* 2008). Other studies agree on the fact that, due to the amount of riverine discharge to these areas and the large CO_2 emissions observed in inner estuaries, salt marshes and mangroves, continental margins behave more as CO_2 sources (Frankignoulle *et al.* 1998; Laruelle *et al.* 2010). Chen and Borges (2009) proposed a reconciliation between these opposing views, where continental shelves act as sinks and near-shore ecosystems as sources of atmospheric CO_2. Still, the role of the coastal oceans as sources or sinks of CO_2 is still under debate (Friederich *et al.* 2008; Chen and Borges 2009; Laruelle *et al.* 2010).

Long-time series observations made in waters along the Pacific coast of North America illustrate how widely coastal water CO_2 fluxes vary in space and time, driven by factors such as upwelling and relaxation (Friederich *et al.* 2002; Evans

et al. 2011) or seasonal changes in seawater temperature (Takahashi *et al.* 1993; Chavez *et al.* 2007). An analysis of half a million measurements of sea-air CO_2 flux in North America, suggested that coastal oceans at lower latitudes tend to be sources of CO_2 to the atmosphere, while the ones located at higher latitudes tend to be sinks (Chavez *et al.* 2007). These sea-air fluxes vary according to large-scale climate oscillations such as El Niño and the Pacific Decadal Oscillation (PDO) (Chavez *et al.* 1999; Friederich *et al.* 2002), which alter the oceanic CO_2 sink/source conditions through seawater temperature changes, as well as ecosystem variations that occur through physical-biological interactions (Takahashi *et al.* 2002; Patra *et al.* 2005).

Based on the previous work by Chavez et al. (2007), an extensive pCO_2 data set was put together by merging the MBARI and LDEO-CDIAC $pCO_{2\ sw}$ databases. The difference between the oceanic and atmospheric pCO_2 values located within the first 100 km from shore were used to calculate CO_2 fluxes from Canada to Chile. This approach allows us to relate the pCO_2 dynamics in the eastern Pacific coast to other parameters such as preformed nutrient availability, seasonal coastal upwelling, biological activity, wind strength, riverine discharge (Friederich *et al.* 2002, 2008; Hales *et al.* 2005; Evans *et al.* 2011) or depth of the oxygen minimum zone (Stramma *et al.* 2008), which vary along the eastern Pacific coast.

MATERIALS AND METHODS

In order to explore the patterns in the seawater pCO_2 (pCO_{2sw}) over the Pacific Coast of the Americas, from Vancouver (British Columbia, Canada) to the tip of South America (Punta Arenas, Chile), a large pCO_2 dataset was put together. Various sources were used for the extraction of seawater and atmospheric pCO_2, wind speed and coastline data (Table 1), which will be further explained.

Table 1. Datasets used in the calculations of the CO_2 system

Dataset	Description
LDEO CDIAC	Seawater pCO_2 data offered by the Carbon Dioxide Information Analysis Center (CDIAC), Oak Ridge National Laboratory, U.S. Department of Energy, Oak Ridge, Tennessee. See (Takahashi *et al.* 2007) for detailed information on the data gathering, and at the website http://cdiac.ornl.gov/oceans/LDEO_Underway_Database/index.html.
MBARI	Seawater pCO_2 data was obtained from the underway system maintained by the Biological Oceanography Group at MBARI. It was gathered from shipboard underway xCO_2 measurement systems at different locations and between 1993 – 2008.
Global View	Atmospheric pCO_2 was downloaded from Globalview via anonymous FTP, at ftp.cmdl.noaa.gov/ccg/co2/GLOBALVIEW. See (Globalview-CO2 2012) for more details.
Wind speed	The wind speed data used corresponds to the NCEP Blended wind data set. See (Zhang *et al.* 2006) for detailed information. Data information can be found in http://www.ncdc.noaa.gov/oa/rsad/air-sea/seawinds.html
Coastline data	The coastline data from the Pacific coast of the Americas was extracted from http://www.ngdc.noaa.gov/mgg/coast

SEAWATER pCO_2 DATASET

The pCO_{2sw} datasets were extracted from two sources: the Monterey Bay Aquarium Research Institute (MBARI) and the Lamont Doherty Earth Observatory – Carbon Dioxide Information Analysis Center (LDEO-CDIAC). Each dataset is a compilation from different projects and sources. The MBARI

database provided information from Vancouver to Chile, while the LDEO-CDIAC database covered a region further south on the Pacific coast of South America (Figure 2).

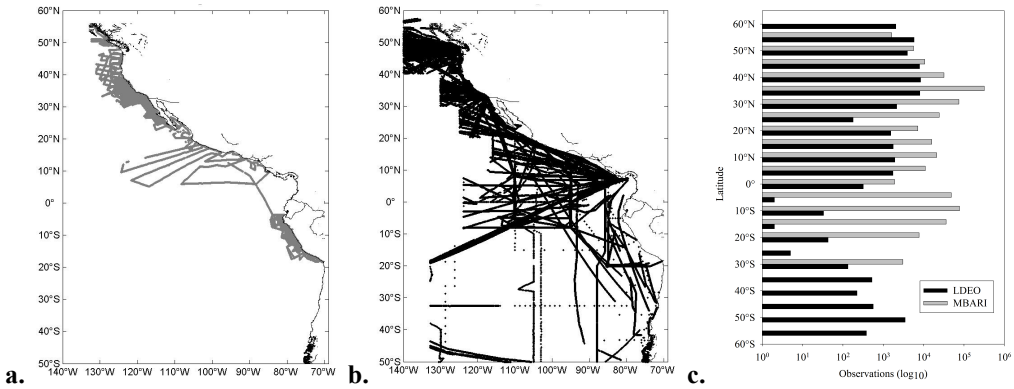

Figure 2. a. MBARI and **b.** LDEO cruises included in the $pCO_{2\,sw}$ databases. **c.** Number of coastal ocean observations included in the CO_2 flux calculations. Black and grey bars correspond to LDEO and MBARI observations, respectively.

LDEO-CDIAC dataset

The LDEO-CDIAC data set is a very large collection of pCO_2 available free of charge as a numeric data package (NDP). The NDP consists of the oceanographic data files and printed documentation, which describe the procedures and methods used to obtain data. (Takahashi *et al.* 2007) extensively describe the measurements and calculations performed to obtain the seawater pCO_2 of the LDEO-CDIAC database (refer to it for detailed information on this database).

The 2007 version of this database was available at the moment of data processing, listing more than 4.1 million measurements of surface water pCO_2 obtained over the global oceans from 1968 to 2007 (including open ocean and coastal water measurements). The data assembled include only those measured by equilibrator-CO_2 analyzer systems and have been quality-controlled based on the stability of the system performance, the reliability of calibrations for CO_2 analysis, and internal consistency of the data. The overall uncertainty for the pCO_2 values listed is estimated to be ± 2.5 µatm on average (Takahashi *et al.* 2007).

The seawater pCO_2 data listed in the LDEO-CDIAC database are based on direct seawater pCO_2 measurements made using equilibrator-CO_2 analyzer systems (Takahashi *et al.* 2007). Using the reported CO_2 concentration values, the pCO_2 in sample seawater at equilibration temperature ($pCO_{2\ sw@Tequi}$) was recomputed as

$$pCO_{2\ sw@T_{equi}} = xCO_{2\ sw} * \left(P_{equi} - P_{water}\right) \qquad \text{Equation 1}$$

where $xCO_{2\ sw}$ is the mole fraction of CO_2 in the carrier gas, P_{equi} is the total pressure of gas in the equilibrator, and P_{water} is the equilibrium water vapor pressure at temperature of equilibration (T_{equi}) and salinity.

The pCO_2 at *in situ* seawater temperature was computed using an integrated form of the temperature effect for isochemical seawater, $\left(\frac{\partial lnpCO_2}{\partial T}\right)_{Sal,Alk,TCO_2}$, described by (Takahashi *et al.* 1993):

$$pCO_{2\ sw@T_{in\ situ}} = pCO_{2\ sw@T_{equi}} * exp\left\{0.0433 * \left(T_{in\ situ} - T_{equi}\right) - 4.35\times10^{-5} * \left[(T_{in\ situ})^2 - \left(T_{equi}\right)^2\right]\right\} \qquad \text{Equation 2}$$

The LDEO-CDIAC dataset is a very large collection of pCO_2. As the data is available in Ocean Data View (ODV) format, this program was used to extract smaller subsets of data near the coast using the graphic spline function. These subsets were then merged and further processed to extract locations 400 km from the coast; pCO_2 data were further filtered to analyze the 100 km offshore bin.

MBARI dataset

The seawater pCO_2 dataset of MBARI was gathered using shipboard underway xCO_2 measurement systems, which are designed for rapid deployment and semi-autonomous operation. A Licor 6262 CO_2/H_2O analyzer coupled to a membrane gas contactor and a custom gas flow control module was used. Data was collected every two seconds and processed data was recorded as one minute averages. Calibrations were performed every two hours with three running standards (0 ppm, near atmospheric ppm, and near atmospheric + 100 ppm) that were referenced to six Earth System Research Laboratory (ESRL) standards (ranging from 240 ppm to 1200 ppm).

MBARI CO_2 data was available as the mole fraction of CO_2 in dry air (xCO_2), while LDEO-CDIAC data was presented as the partial pressure of CO_2 (pCO_2). MBARI xCO_2 was converted to pCO_2 using Equation 1, taking in consideration the atmosphere to which the LDEO-CDIAC dataset had been converted. Afterwards, the MBARI and LDEO-CDIAC pCO_2 datasets were combined to produce a large final pCO_2 dataset of ~10^6 observations (Figure 2).

After pCO_2 calculations, temperature sensors were cross-calibrated with Seabird temperature probes to ±0.01ºC. Temperature normalization was done with Equation 3.

$$pCO_{2@Tn} = pCO_{2@To} * exp\big(0.0423 * (T_n - T_o)\big) \qquad \text{Equation 3}$$

where $pCO_{2@Tn}$ and $pCO_{2@To}$ are the pCO_2 at the new temperature (T_n = 15ºC) and pCO_2 at the original temperature (T_o), respectively. This dataset was filtered to extract pCO_2 data in locations 400 km from coast; pCO_2 data were further filtered to 100 km offshore bins.

ATMOSPHERIC pCO_2 DATASET

GLOBALVIEW-CO_2 is a product of the Cooperative Atmospheric Data Integration Project that uses discrete and quasi-continuous measurements from fixed surface and tower sites, moving ships and aircraft sites. The atmospheric pCO_2 ($pCO_{2\ atm}$) dataset was downloaded from the internet via anonymous FTP ((Takahashi *et al.* 2007)ftp.cmdl.noaa.gov/ccg/co2/GLOBALVIEW). Discrete samples are collected *in situ* at weekly to monthly intervals and returned to the collaborating measurement laboratory for analysis. Quasi-continuous samples are measured *in situ* and are preprocessed to produce a single value per day. The collaborating laboratories often perform this averaging process, using well-established, previously published methods. In some instances, the averaging is done at ESRL in cooperation with the contributing laboratories (Globalview-CO2 2012).

The extraction of the appropriate $pCO_{2\ atm}$ value from the Global View dataset was done selecting one of three locations: Cape Meares (Oregon, United States. Acronym: CMO. Position: 45.48ºN, 123.97ºW), Christmas Island (Republic of Kiribati. Acronym: CHR. Position: 1.70ºN, 157.17ºW) or Easter Island (Chile. Acronym: EIC. Position: 27.15ºS, 109.45ºW). Each seawater pCO_2 data point was matched by year, month, and day to the corresponding atmospheric pCO_2 value. This enabled the calculation of the difference between seawater and atmospheric pCO_2, which is used in the CO_2 flux calculations.

WIND SPEED DATASET

The Blended Sea Winds web page of the NOAA Satellite and Information Service (http://www.ncdc.noaa.gov/oa/rsad/air-sea/seawinds.html) contains globally gridded, high resolution ocean surface vector winds and wind stresses on a global 0.25° grid, as well as multiple time resolutions of 6-hourly, daily (averages in time of the 6-hourly data), monthly (provided as averages of the daily fields), and 11-year (1995-2005) climatological monthlies. The wind speeds are generated by

blending observations from multiple satellites (up to six since June 2002, including scatterometers (QuikSCAT), SSMIs, TMI and AMSR-E; Figure 1 in (Zhang *et al.* 2006)).

Monthly wind speed data was extracted from the NCEP blended wind data set and was matched by year, month and 0.25º-binned latitude and longitude locations, to the seawater pCO_2 data.

CO_2 FLUX CALCULATIONS

The net sea-air CO_2 flux (FCO_2, in mol m^{-2} yr^{-1}) was estimated using the difference between sea water and atmospheric pCO_2 (ΔpCO_2, Equation 4), the sea-air gas transfer rate (k, in cm h^{-1}) parameterized as a function of squared wind speed (Wanninkhof 1992), the CO_2 solubility in seawater (S, in mol kg^{-1} atm^{-1}) calculated from (Weiss 1974), and a unit conversion factor of 0.24.

$$\Delta pCO_2 = pCO_{2\,sw} - pCO_{2\,atm} \qquad \text{Equation 4}$$

$$FCO_2 = k * S * \Delta pCO_2 * 0.24 \qquad \text{Equation 5}$$

Final averaging was done by cruise and by 5-degree latitudinal bin. Fluxes were calculated for each observation, and were later averaged by cruise and 5-degree latitudinal bin as well.

NUTRIENT CONTENT OF SURFACE WATERS

Preformed nitrate is the nitrate originally present in a water mass when it leaves the ocean surface (Johnson *et al.* 2010), prior to *in situ* organic matter respiration (Emerson and Hayward 1995; Abell *et al.* 2005). Previous works conducted in some parts of the eastern Pacific coast have observed the importance of preformed

nutrient availability (and nitrate in particular) on the pCO_2 content of recently upwelled waters (Hales *et al.* 2005; Friederich *et al.* 2008).

In order to explain the ΔpCO_2 values found, we correlated preformed nitrate with ΔpCO_2 calculated for surface waters. Based on these results, we developed a simple model that allowed us to calculate values of $pCO_{2\ sw}$ under three different scenarios of nutrient utilization. The equations used to calculate the variables of the CO2 system are shown in Table 2.

Initial conditions

Our starting point was a hypothetical water mass forming at high latitudes with a pCO_2 content ($pCO_{2\ pre}$) of 370 ppm, under the assumption that this was the atmospheric CO_2 concentration at the time of water mass formation, and that complete equilibrium between the ocean surface and the atmosphere had been achieved prior to its sinking (Table 2). For the calculation of the nitrate content ($NO_{3\ pre}$) of this initial water mass, we assumed that the $\Delta O_2/\Delta NO_3^-$ ratio was constant and that the waters were saturated with respect to oxygen when at ocean surface (Emerson and Hayward 1995). We calculated $NO_{3\ pre}$ from nitrate measured at 50 m ($NO_{3\ 50m}$), Apparent Oxygen Utilization at 50 m (AOU_{50m}) and a N:O = 0.11 (Redfield *et al.* 1963). In order to obtain surface total alkalinity values for this initial water mass, we had to calculate total alkalinity values at 50 m depth ($TAlk_{50m}$); these were calculated from a linear relationship between salinity and alkalinity obtained from surface to 50 m WOCE data (Table 2). Total alkalinity values of the initial water mass ($TAlk_{pre}$) were calculated from $TAlk_{50m}$, AOU_{50m} and a N:O = 0.11 (Redfield *et al.* 1963). For $NO_{3\ 50m}$ and $TAlk_{50m}$ we assumed that no mixing or dilution with adjacent water masses occurred, and thus salinity was taken as a conservative variable from surface to 50 m.

Table 2. Equations used in our model. [1.] For initial conditions, a stoichiometric ratio of oxygen consumption to nitrate regeneration N:O = 0.11 was used (Redfield *et al.* 1963). [2.] Relationship between alkalinity and salinity registered in WOCE, for data between surface and 50 m (G. Friederich, *pers. comm.*). [3.] For waters at 50 m depth and positive or negative $NO_{3\ pre}$, a stoichiometric ratio of oxygen consumption to carbon regeneration C:O = 0.77 was used ((Redfield *et al.* 1963). [4.] For waters at 50 m depth and negative $NO_{3\ pre}$, a stoichiometric ratio of nitrate consumption to carbon regeneration C:N ≈ 1.1 was used (Paulmier *et al.* 2009). [5.] In surface waters, a stoichiometric ratio of nitrate consumption to carbon regeneration C:N = 6.6 was used (Redfield *et al.* 1963).

Initial conditions	$pCO_{2\ pre}$	370 ppm
	$NO_{3\ pre}$	$NO_{3\ 50m} - AOU_{50m} * N{:}O^{1}$
	$TAlk_{pre}$	$TAlk_{50m} + AOU_{50m} * N{:}O^{1}$
	$TCO_{2\ pre}$	$f(pCO_{2\ pre,} TAlk_{pre}, S_{50m}, T_{50m})$
	pH_{pre}	$f(pCO_{2\ pre,} TAlk_{pre}, S_{50m}, T_{50m})$
Source water	$pCO_{2\ 50m}$	$f(TCO_{2\ 50m,} TAlk_{50m}, S_{50m}, T_{50m})$
	$NO_{3\ 50m}$	WOA
	$TAlk_{50m}$	$60.2 * S\ + 205.5^{2}$
	$TCO_{2\ 50m}$	$TCO_{2\ pre} + AOU_{50m} * C{:}O^{3} + denitC$ *denitC* = 0 if $NO_{3\ pre}$ is positive, $denitC\ = [-NO_{3\ pre}] * C{:}N^{4}$ if $NO_{3\ pre}$ is negative
	pH_{50m}	$f(TCO_{2\ 50m,} TAlk_{50m}, S_{50m}, T_{50m})$
Upwelled water	$pCO_{2\ surf}$	$f(TCO_{2\ surf,} TAlk_{surf}, S_{surf}, T_{surf})$
	$TAlk_{surf}$	$TAlk_{pre} + \Delta N$
	$TCO_{2\ surf}$	$TCO_{2\ pre} - \Delta N * C{:}N^{5} + denitC$
	pH_{surf}	$f(TCO_{2\ surf,} TAlk_{surf}, S_{surf}, T_{surf})$
	$pCO_{2\ surf}$	$f(TCO_{2\ surf,} TAlk_{surf}, S_{surf}, T_{surf})$
1. No biology	ΔN	$NO_{3\ pre} - NO_{3\ 50m}$
2. Full biology		$NO_{3\ pre}$
3. Observed biology		$NO_{3\ pre} - NO_{3\ surf}$

Preformed total inorganic CO_2 ($TCO_{2\ pre}$) and pH_{pre} were calculated as functions of $pCO_{2\ pre}$, $TAlk_{pre}$, salinity and temperature at 50 m (S_{50m} and T_{50m}) using the CO_2 system calculations (CO2SYS). This program relates parameters of the carbon dioxide system in seawater and freshwater, using two of the four

measurable variables (TAlk, TCO_2, pH, and either fugacity (fCO_2) or pCO_2), to calculate the other two parameters at a set of input conditions (temperature and pressure) and a set of output conditions chosen by the user (Lewis and Wallace 1998).

Source water

We assume that the hypothetical water mass sinks to a depth of 50m (this is the depth at which the water mass is located prior to upwelling). The total inorganic carbon present in this water mass ($TCO_{2\ 50m}$) was calculated based on increases of $TCO_{2\ pre}$ due to remineralization of organic matter. As AOU represents the biological activity that the water mass has experienced since it was last in equilibrium with the atmosphere, it is used in the calculation of this increase, with a C:O = 0.77 (Redfield *et al.* 1963). Additional increases due to denitrification were taken into account in the calculation of $TCO_{2\ 50m}$, basically when $NO_{3\ pre}$ was negative. In this case we added the absolute value of $NO_{3\ pre}$ concentration with a C:N ratio of 1.1, following Paulmier *et al.* (2009). $pCO_{2\ 50m}$ and pH_{50m} were calculated as functions of $TAlk_{50m}$, $TCO_{2\ 50m}$, S_{50m} and T_{50m}, using CO2SYS.

Upwelled water

Upwelling of the 50 m water mass at low latitudes brings cold and nutrient rich waters to the surface, with high levels of CO_2 and nitrate. In the presence of light, nitrate and CO_2 are photosynthesized to form organic compounds. We developed a simple model in which we calculate the final set of CO_2 variables after upwelling under three different scenarios: a) none of the upwelled nutrients are used (no nutrient utilization scenario), b) nutrients are depleted at surface (full nutrient utilization scenario), and c) we use the observed nutrients in surface for the calculations (observed nutrient utilization scenario). In the first scenario we assumed that no photosynthesis is taking place and that all variation in CO_2 is due to the thermodynamical effect of temperature on CO_2, and to the difference between $NO_{3\ pre}$ and $NO_{3\ 50m}$. On the second scenario, we considered that phytoplankton consumed all the available nutrients and that $NO_{3\ pre}$ utilization

increases TAlk while decreasing TCO_2. For the third scenario, we considered that the difference between $NO_{3\ pre}$ and $NO_{3\ 50m}$, which account for nutrient utilization, would account for changes in alkalinity and TOC_2 measured in surface.

RESULTS

By combining the LDEO-CDIAC and MBARI databases, the study area was expanded to regions were one of either database didn't have enough observations. For example: MBARI doesn't have observations in the southern hemisphere, so this cruises were supplied by LDEO-CDIAC. On the other hand, MBARI has a lot more cruises than LDEO-CDICA near the equator. A final dataset close to one million observations was produced, with more cruises found between 30ºN and 35ºN, followed by data found at 10ºS. The lowest number of observations was found in the southern hemisphere at 25ºS (Figure 2c).

pCO_2 AND CO_2 FLUX CALCULATIONS

pCO_2 undersaturation of surface waters occurred in high latitudinal waters (Figure 3a) of both hemispheres, with a little more undersaturation found in the southern hemisphere (between 40ºS and 55ºS, ΔpCO_2 values ranged from -50 to -86 µatm). Between 40ºN and 60ºN, ΔpCO_2 varied from -55 to -80 µatm, with the highest undersaturation found at 55ºN. On the other hand, oversaturation of seawater pCO_2 was found in low latitudinal waters between 25ºN and 35ºS. The highest oversaturation was found between 5ºS and 15ºS, with ΔpCO_2 values exceeding +150 µatm (Figure 3a).

Higher wind speeds where found at high southern latitudes, with values as low as 8 m/s at 40ºS and as high as 11 m/s at 55ºS. Even though wind speeds at high northern latitudes were higher than the average found for the western coast of the Americas, they were slower than those found for the southern hemisphere, with values just approaching 7 m/s in latitudes higher than 40ºN. On the other hand,

lower than average wind speeds (6.5 m/s) were found between 35ºN and 20ºS (Figure 3b).

CO_2 flux calculations yielded negative values (flux into the ocean) in waters between 45ºN and 60ºN, and between 40ºS and 55ºS (Figure 3c), with the highest influx at high southern latitudes (-9.2 and -7.1 moles C m^{-2} y^{-1} at 55ºS and 50ºS, respectively). On the contrary, fluxes from the ocean to the atmosphere were found around the Baja California upwelling system at 25ºN, and in the Peruvian and Chilean upwelling systems, between 5ºS and 35ºS. The highest emission values were found at 5ºS (4.4 moles C m^{-2} y^{-1}) followed by fluxes at 30ºS (3.5 moles C m^{-2} y^{-1}). Near-neutral fluxes were found at 45ºS (-0.8 moles C m^{-2} y^{-1}), 20ºS (0.6 moles C m^{-2} y^{-1}), from the equator to 20ºN (from -0.2 to 0.5 moles C m^{-2} y^{-1}), from 30ºN to 40ºN (-0.3 to 0.5 moles C m^{-2} y^{-1}), and at 50ºN (0.4 moles C m^{-2} y^{-1}).

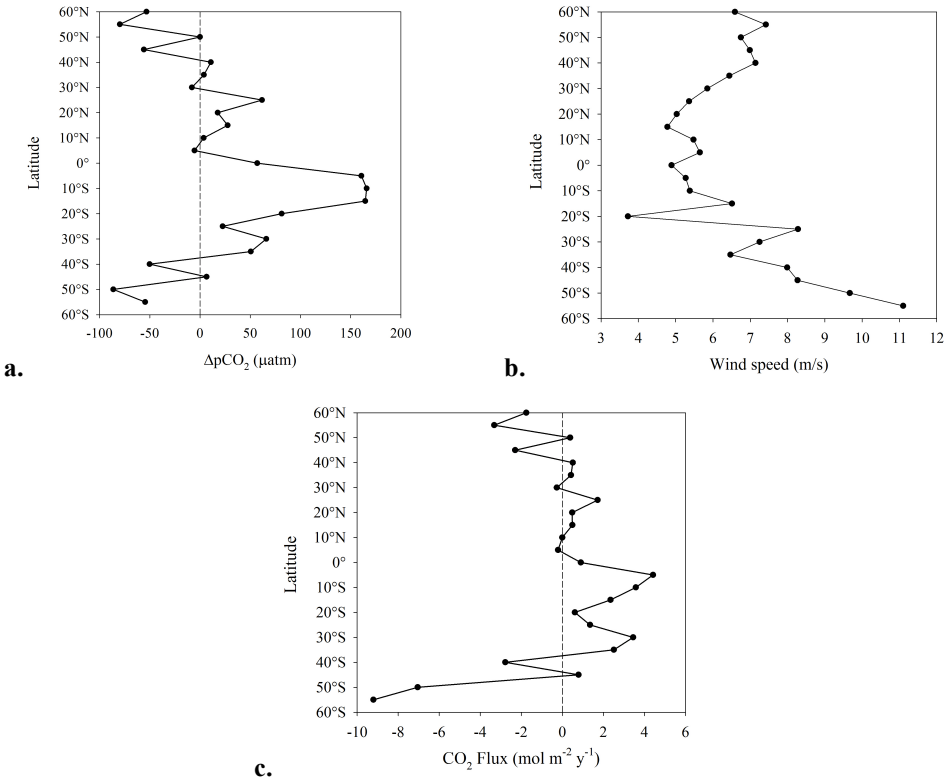

Figure 3. a. ΔpCO_2 values found for the Pacific coast of the Americas, from 60ºN to 55ºS. **b.** Wind speed calculated from the NCEP blended wind data set for the eastern Pacific coast. **c.** Flux calculations obtained from the combination of LDEO-CDIAC and MBARI pCO_2 databases.

NITRATE AND PARAMETERS OF THE CO_2 SYSTEM IN DIFFERENT SCENARIOS OF CLIMATE CHANGE

A strong negative correlation between preformed nitrate and ΔpCO_2 was found ($r = -0.71$, $p < 0.05$, Figure 4a), meaning that waters with positive preformed nitrate are more undersaturated with pCO_2 when compared to waters with near zero or negative preformed nitrate. This coincides with the ΔpCO_2 distribution found for the western coast of the Americas (Figure 4b), in which surface waters at high latitudes have higher preformed nitrate and are more undersaturated with CO_2 than the ones located near to the equator.

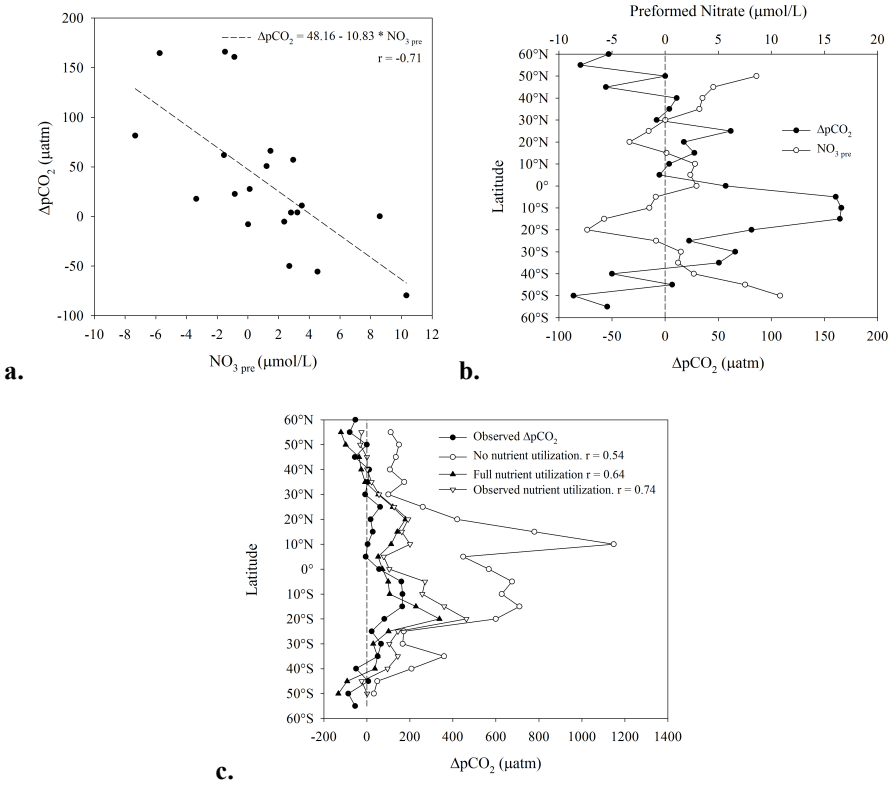

Figure 4. a. Correlation between preformed nitrate and ΔpCO_2 ($r = -0.71$, $p < 0.05$) **b.** Distribution of observed ΔpCO_2 values (black circles) and preformed nitrate values (open circles) along the western coast of the Americas, from 60ºN to 55ºS. **c.** ΔpCO_2 obtained for three nutrient utilization scenarios: no nutrient utilization (white circles), full nutrient utilization (black triangles) and observed nutrient utilization (white upside down triangles). The observed ΔpCO_2 is shown in black circles.

Calculated ΔpCO_2 for the different nutrient utilization scenarios showed that when no nutrients were used ΔpCO_2 rose to maximum levels; values were especially

higher in areas surrounding the equator, reaching 1200 µatm at 10ºN. On the other hand, when nutrients were depleted, ΔpCO_2 values were lowered to the minimum. When calculating ΔpCO_2 in the observed nutrient utilization scenario, ΔpCO_2 values were intermediate between those calculated with methods 1 and 2. The correlation between our CO_2 disequilibrium and the ones calculated for each of the different nutrient utilizations scenarios, showed a higher correlation with the observed nutrient utilization ($r = 0.74$, $p<0.05$, Figure 4).

DISCUSSION

PARAMETERS OF THE CO_2 SYSTEM

The CO_2 flux calculations resembled those of ΔpCO_2 values, *i.e.* influx at high latitudes and outgassing around the equator. However, the strong ΔpCO_2 values found for some latitudinal bins were not transformed into stronger fluxes, compared to regions with weaker ΔpCO_2 values. Latitudinal bins south of the equator yielded the highest ΔpCO_2 values, surpassing +150 ppm. CO_2 fluxes calculated for this region (5ºS-15ºS) ranged between 2.35 and 4.42 moles C m^{-2} y^{-1}. On the other hand, southern latitudes (30ºS and 35ºS) with ΔpCO_2 values of +66 and +51 ppm, yielded flux values of 3.45 and 2.51 moles C m^{-2} y^{-1}, which aren't as low as expected from the ΔpCO_2 values. The lack of correspondence between high ΔpCO_2 values and high CO_2 fluxes is due to the wind variation along the eastern Pacific coast, where wind speeds are higher at high latitudes. More CO_2 exchange would occur were more turbulence is generated from high-speed winds.

The high outfluxes found at 5ºS and 30ºS correspond to the Peruvian and Chilean upwelling systems, located in the southern tropical Pacific. They are known to be sources of CO_2 to the atmosphere throughout the year (Friederich *et al.* 2008). Outfluxes located at 45ºS correspond to the Oregon coast, that has been considered as a sink for atmospheric CO_2 by Hales *et al.* (2005). High latitudinal waters are strong sinks for atmospheric CO_2 due to low temperatures increasing CO_2 solubility, as well as high wind speeds that increase turbulence and enhance the CO_2 exchange in the ocean surface. Low latitudinal waters are sources of CO_2

to the atmosphere due to higher temperatures that decrease CO_2 solubility and stronger upwelling systems located near the equator.

HOW WILL NITRATE AVAILABILITY AFFECT PARAMETERS OF THE CO_2 SYSTEM IN DIFFERENT SCENARIOS OF CLIMATE CHANGE?

Understanding the mechanisms that supply nutrients to the shallowest layer of the ocean, where most net community production occurs is critical to develop the capability to predict the response of ocean ecosystems to a changing climate (Johnson *et al.* 2010). In waters that form in regions with measurable surface nutrients, respiration of nitrogen-poor DOM reduces the preformed nitrate concentration, while it results in negative preformed nitrate in waters that formed where surface nutrients were depleted (Emerson and Hayward 1995). The layer of negative preformed nitrate is a depth zone where respiration is taking place without the stoichiometric component of nitrogen remineralization. Emerson and Hayward (1995) proposed that nitrogen-poor dissolved organic matter could be an important respiration substrate in these regions and that its degradation may be accompanied by very little dissolved nitrogen release or even nitrate uptake. The high NO_3^- tongue spreading west from Central America along 20ºN, and west from South America at 20ºS is not within the ventilated water but owes its high nutrient levels to the oxygen minimum, which is formed, at least partially, by the lack of ventilation in this location. The westward extension is due to the flow of the North Equatorial Current (Emerson and Hayward 1995).

Negative $NO_{3\ pre}$ below the mixed layer results if nitrate is assimilated into biomass and a corresponding amount of oxygen is not produced, or if oxygen is consumed and nitrate is not produced (Johnson *et al.* 2010). Positive preformed nitrate values are not uniquely due to greater-than-zero surface nitrate values; they could also originate from surface water oxygen supersaturation or smaller $\Delta O_2/\Delta NO_3^-$ ratios tan expected (Emerson and Hayward 1995). Near zero preformed nitrate values originate when the nitrate concentration is equal to the

term -(AOU)/R. If they are both near zero, it means that the waters have been in frequent contact with the surface ocean where nutrient concentrations are low. If NO_3^- = -(AOU)/R and they are nonzero numbers, then the bulk of the nitrate originates from local respiration of organic matter (Emerson and Hayward 1995)

The high correlation between preformed nitrate and ΔpCO_2 reaffirms the theory that water masses containing more preformed nitrate will present lower surface pCO_2, which in turn will result in negative or low ΔpCO_2 values, meaning that they can absorb more atmospheric pCO_2. Consumption of nutrients should return pCO_2 to atmospheric levels, and additional consumption of the $NO_{3\ pre}$ can then produce an additional carbon drawdown (Friederich *et al.* 2008). When applying this theory to the results obtained in three nutrient utilization scenarios, the higher ΔpCO_2 value obtained corresponded to the one where no nutrients were being used. If photosynthesis was stopped or slowed due to climate change effects, regions such as the tropics that lack preformed nutrients would exhibit large excess in CO2 in upwelled waters. This would lower seawater pH and thus increase the effects of ocean acidification, particularly in water masses surrounding the equator.

CONCLUSIONS/RECOMMENDATIONS

Undersaturation of ΔpCO_2 was obtained in high latitudes of the western coast of the Americas, whereas oversaturation was obtained in a region south of the equator. Strong fluxes into the ocean were also obtained at high latitudes; higher influxes in the southern hemisphere were due to higher wind speeds calculated for this region. Through a simple model we were able to relate preformed nitrate values of the western coast of the Americas to the ΔpCO_2 pattern obtained from the combination of two large databases. This correlation was strong and negative, meaning that surface waters containing high preformed nitrate values in their formation were able to draw down surface pCO_2 much more than waters formed in regions were little or no nutrients were measured at surface. Waters

surrounding the tropics have little or negative preformed nitrate values, which explains the ΔpCO_2 found in this region. The results of the model also showed that when no nutrients are being used in surface, CO_2 isn't being incorporated into phytoplankton and the biological pump. Preformed nitrate can be used as a proxy of climate change scenarios in which if photosynthesis was stopped, or phytoplankton decreased due to the effects of global warming and/or ocean acidification, the excess of surface CO_2 would translate into decrease of pH which would intensify levels ocean acidification. The tropical Pacific would be the regions suffer these effects, compared to the rest of the western coast of the Americas.

ACKNOWLEDGEMENTS

I would like to thank the David and Lucile Packard Foundation and the Monterey Bay Aquarium Research Institute for funding this internship; it is a wonderful experience to be part of the MBARI staff, at least for the summer! I also want to thank my mentor, Francisco Chavez, for giving me the possibility of coming to work in his lab once again. He doesn't quite understand how grateful I am and what a big deal this is for me!!! I also wouldn't have been able to know MBARI in the first place if it weren't for my research institutions back in Spain: the Marine Research Institute in Vigo (IIM) that belongs to the Spanish National Research Council (CSIC); I hope that better times lie ahead, in terms of research funding. I also want to thank Gernot Friederich, Monique Messiè and Reiko Michisaki from the Biological Oceanography Group in MBARI for all their help during data processing; Monique for all those Matlab lessons I am sure are going to pay off in the near future (keep in mind I will e-mail you!), Reiko for so many scares I gave you regarding data processing and for going back to search for her old lab notes in order to answer my questions; and Gernot for making his best effort in explaining the way the variables in the CO_2 system behave. Jules Friederich and Chris Wahl, for showing me the way around the lab and for letting me hang around their work place just watching them work, and asking them all

sorts of questions regarding their instruments and voltages. Tim Pennington and Marguerite Blum, thanks for all the daily cruises, for showing me the sampling dynamics; to Marguerite, thanks for all your patience in showing me the way around the "Dungeon Lab" and for sharing your pCO_2 processing notes with me. Special thanks to George Matsumoto and Linda Kuhnz for your wonderful work with the interns; you really keep us busy and make our stay very enjoyable! And last but not least… thanks to the wonderful 2013 MBARI interns… you guys have been awesome and I am really happy I had the opportunity of sharing this wonderful experience with you guys. Life has great things ahead for every one of us; just remember that! Love you guys!

♬ *And we danced, and we cried, and we laughed, and had a really, really, really good time* ♬

References

Abell, J., Emerson, S. and Keil, R.G. (2005) Using preformed nitrate to infer decadal changes in DOM remineralization in the subtropical North Pacific. *Global Biogeochemical Cycles* **19**, GB1008.

Chavez, F.P., Strutton, P.G., Friederich, G.E., Feely, R.A., Feldman, G.C., Foley, D.G. and McPhaden, M.J. (1999) Biological and Chemical Response of the Equatorial Pacific Ocean to the 1997-98 El Niño. *Science* **286**, 2126–2131.

Chavez, F.P., Takahashi, T., Friederich, G., Hales, B., Wanninkhof, R. and Feely, R.A. (2007) Chapter 15. Coastal oceans. In: *The First State of the Carbon Cycle Report (SOCCR): The North American Carbon Budget and Implications for the Global Carbon Cycle. A Report by the U.S. Climate Change Science Program and the Subcommittee on Global Change Research.* (eds A.W. King, L. Dilling, G.P. Zimmerman, *et al.*). National Oceanic and Atmospheric Administration, National Climatic Data Center, Asheville, NC, USA., pp 157–166.

Chen, C.-T.A. and Borges, A.V. (2009) Reconciling opposing views on carbon cycling in the coastal ocean: Continental shelves as sinks and near-shore ecosystems as sources of atmospheric CO2. *Deep Sea Research Part II: Topical Studies in Oceanography* **56**, 578–590.

Cobo-Viveros, A.M., Padin, X.A., Otero, P., de La Paz, M., Ruiz-Villarreal, M., Ríos, A.F. and Pérez, F.F. (2013) Short-term variability of surface carbon dioxide and sea-air CO2 fluxes in the shelf waters of the Galician coastal upwelling system. *Scientia Marina*, 1–12.

Emerson, S. and Hayward, T.L. (1995) Chemical tracers of biological processes in shallow waters of North Pacific: Preformed nitrate distributions. *Journal of Marine Research* **53**, 499–513.

Evans, W., Hales, B. and Strutton, P.G. (2011) Seasonal cycle of surface ocean pCO2 on the Oregon shelf. *Journal of Geophysical Research* **116**, 11pp.

Feely, R., Doney, S. and Cooley, S. (2009) Ocean Acidification: Present Conditions and Future Changes in a High-CO2 World. *Oceanography* **22**, 36–47.

Frankignoulle, M., Abril, G., Borges, A., *et al.* (1998) Carbon Dioxide Emission from European Estuaries. *Science* **282**, 434–436.

Friederich, G.E., Ledesma, J., Ulloa, O. and Chavez, F.P. (2008) Air–sea carbon dioxide fluxes in the coastal southeastern tropical Pacific. *Progress In Oceanography* **79**, 156–166.

Friederich, G.E., Walz, P.M., Burczynski, M.G. and Chavez, F.P. (2002) Inorganic carbon in the central California upwelling system during the 1997–1999 El Niño–La Niña event. *Progress In Oceanography* **54**, 185–203.

Globalview-CO2 (2012) Cooperative Atmospheric Data Integration Project - Carbon Dioxide. NOAA ESRL, Boulder, Colorado [Available at http://esrl.noaa.gov/gmd/ccgg/globalview/]. Available at: http://www.esrl.noaa.gov/gmd/ccgg/globalview/co2/co2_version.html [Accessed October 25, 2011].

Gypens, N., Borges, A.V. and Lancelot, C. (2009) Effect of eutrophication on air–sea CO2 fluxes in the coastal Southern North Sea: a model study of the past 50 years. *Global Change Biology* **15**, 1040–1056.

Hales, B., Takahashi, T. and Bandstra, L. (2005) Atmospheric CO2 uptake by a coastal upwelling system. *Global Biogeochemical Cycles* **19**, 11pp.

IPCC (2007) *Climate Change 2007: The Physical Science Basis. Contribution of Working Group I to the Fourth Assessment Report of the Intergovernmental Panel on Climate Change*, (Vol. 4). Cambridge University Press, Cambridge, United Kingdom and New York, NY, USA.

Johnson, K.S., Riser, S.C. and Karl, D.M. (2010) Nitrate supply from deep to near-surface waters of the North Pacific subtropical gyre. *Nature* **465**, 1062–1065.

Keeling, C.D., Bacastow, R.B., Bainbridge, A.E., Ekdahl, C.A., Guenther, P.R., Waterman, L.S. and Chin, J.F.S. (1976) Atmospheric carbon dioxide variations at Mauna Loa Observatory, Hawaii. *Tellus* **28**, 538–551.

Laruelle, G.G., Dürr, H.H., Slomp, C.P. and Borges, A.V. (2010) Evaluation of sinks and sources of CO2 in the global coastal ocean using a spatially-explicit

typology of estuaries and continental shelves. *Geophysical Research Letters* **37**, 6 PP.

Lewis, E. and Wallace, D. (1998) *Program Developed for CO2 System Calculations*. Environmental Sciences Division, Upton, New York.

Liu, K.-K., Atkinson, L., Chen, C.T.A., *et al.* (2000) Exploring continental margin carbon fluxes on a global scale. *EOS, Transactions American Geophysical Union* **81**, 641–644.

Patra, P.K., Maksyutov, S., Ishizawa, M., Nakazawa, T., Takahashi, T. and Ukita, J. (2005) Interannual and decadal changes in the sea-air CO2 flux from atmospheric CO2 inverse modeling. *Global Biogeochemical Cycles* **19**, 13 PP.

Paulmier, A., Kriest, I. and Oschlies, A. (2009) Stoichiometries of remineralisation and denitrification in global biogeochemical ocean models. *Biogeosciences* **6**, 923–935.

Redfield, A.C., Ketchum, B.H. and Richards, F.A. (1963) The influence of organisms on the composition of sea-water. In: *The composition of sea-water*, Vol. 2. (ed M.N. Hill). John Wiley & Sons, New York, pp 26–77.

Stramma, L., Johnson, G.C., Sprintall, J. and Mohrholz, V. (2008) Expanding Oxygen-Minimum Zones in the Tropical Oceans. *Science* **320**, 655–658.

Takahashi, T., Olafsson, J., Goddard, J.G., Chipman, D.W. and Sutherland, S.C. (1993) Seasonal variation of CO2 and nutrients in the high-latitude surface oceans: A comparative study. *Global Biogeochemical Cycles* **7**, 843–878.

Takahashi, T., Sutherland, S.C. and Kozyr, A. (2007) Global Ocean Surface Water Partial Pressure of CO2 Database: Measurements Performed During 1968-2007 (Version 2007). *ORNL/CDIAC-152, NDP-088a*, 20 pp. Carbon Dioxide Information Analysis Center, Oak Ridge National Laboratory, U.S. Department of Energy, Oak Ridge, Tennessee.

Takahashi, T., Sutherland, S.C., Sweeney, C., *et al.* (2002) Global sea–air CO2 flux based on climatological surface ocean pCO2, and seasonal biological and temperature effects. *Deep Sea Research Part II: Topical Studies in Oceanography* **49**, 1601–1622.

Thoning, K.W., Tans, P.P. and Komhyr, W.D. (1989) Atmospheric carbon dioxide at Mauna Loa Observatory: 2. Analysis of the NOAA GMCC data, 1974–1985. *Journal of Geophysical Research: Atmospheres* **94**, 8549–8565.

Tsunogai, S., Watanabe, S. and Sato, T. (1999) Is there a "continental shelf pump" for the absorption of atmospheric CO2? *Tellus B* **51**, 701–712.

US Department of Commerce, National Oceanic and Atmospheric

Administration, Earth System Research Laboratory and Global Monitoring division (2013) Trends in Carbon Dioxide. Available at: http://www.esrl.noaa.gov/gmd/ccgg/trends/mlo.html [Accessed July 18, 2013].

Wanninkhof, R. (1992) Relationship between wind speed and gas exchange over the ocean. *Journal of Geophysical Research* **97**, 7373–7382.

Weiss, R.F. (1974) Carbon dioxide in water and seawater: the solubility of a non-ideal gas. *Marine Chemistry* **2**, 203–215.

Zhang, H.M., Bates, J.J. and Reynolds, R.W. (2006) Assessment of composite global sampling: Sea surface wind speed. *Geophys. Res. Lett* **33**, L17714.